Nuclear magnetic resonance study on rotational dynamics of water and benzene in a series of ionic liquids: Anion and cation effects.

AUTHOR(S):

Kimura, Hiroshi; Yasaka, Yoshiro; Nakahara, Masaru; Matubayasi, Nobuyuki

CITATION:

Kimura, Hiroshi ...[et al]. Nuclear magnetic resonance study on rotational dynamics of water and benzene in a series of ionic liquids: Anion and cation effects.. The Journal of chemical physics 2012, 137(19): 194503.

ISSUE DATE:

2012-11-21

URL:

http://hdl.handle.net/2433/166069

Nuclear magnetic resonance study on rotational dynamics of water and benzene in a series of ionic liquids: Anion and cation effects

Hiroshi Kimura, Yoshiro Yasaka, Masaru Nakahara, and Nobuyuki Matubayasi

Citation: J. Chem. Phys. **137**, 194503 (2012); doi: 10.1063/1.4766258
View online: http://dx.doi.org/10.1063/1.4766258
View Table of Contents: http://jcp.aip.org/resource/1/JCPSA6/v137/i19
Published by the American Institute of Physics.

THE JOURNAL OF CHEMICAL PHYSICS **137**, 194503 (2012)

Nuclear magnetic resonance study on rotational dynamics of water and benzene in a series of ionic liquids: Anion and cation effects

Hiroshi Kimura,[1] Yoshiro Yasaka,[2] Masaru Nakahara,[1] and Nobuyuki Matubayasi[1,3,a)]
[1]*Institute for Chemical Research, Kyoto University, Uji, Kyoto 611-0011, Japan*
[2]*Department of Molecular Chemistry and Biochemistry, Faculty of Science and Engineering, Doshisha University, Kyotanabe, Kyoto 610-0321, Japan*
[3]*Japan Science and Technology Agency (JST), CREST, Kawaguchi, Saitama 332-0012, Japan and Elements Strategy Initiative for Catalysts and Batteries, Kyoto University, Katsura, Kyoto 615-8520, Japan*

(Received 24 September 2012; accepted 22 October 2012; published online 21 November 2012)

The rotational correlation times (τ_{2R}) for polar water (D_2O) molecule and apolar benzene (C_6D_6) molecule were determined in ionic liquids (ILs) by means of the ^{2}H (D) NMR spin-lattice relaxation time (T_1) measurements. The solvent IL was systematically varied to elucidate the anion and cation effects separately. Five species, bis(trifluoromethylsulfonyl)imide ($TFSI^-$), trifluoromethylsulfonate (TfO^-), hexafluorophosphate (PF_6^-), chloride (Cl^-), and formate ($HCOO^-$), were examined for the anion effect against a fixed cation species of 1-butyl-3-methyl-imidazolium ($bmim^+$). Four species, $bmim^+$, *N*-methyl-*N*-butylpyrrolidinium ($bmpy^+$), *N*,*N*,*N*-trimethyl-*N*-propylammonium ($N_{1,1,1,3}^+$), and *P*,*P*,*P*-trihexyl-*P*-tetradecylphosphonium ($P_{6,6,6,14}^+$), were employed for the cation effect against a fixed anion species of $TFSI^-$. The τ_{2R} ratio of water to benzene, expressed as $\tau_{W/B}$, was used as a probe to characterize the strength of Coulombic solute-solvent interaction in ILs beyond the hydrodynamic limit based on the excluded-volume effect. The $\tau_{W/B}$ value was found to strongly depend on the anion species, and the solute dynamics are sensitive not only to the size but also to the chemical structure of the component anion. The cation effect was rather weak, in contrast. The largest and most hydrophobic $P_{6,6,6,14}^+$ cation was exceptional and a large $\tau_{W/B}$ was observed, indicating a unique solvation structure in [$P_{6,6,6,14}^+$]-based ILs. © *2012 American Institute of Physics*. [http://dx.doi.org/10.1063/1.4766258]

I. INTRODUCTION

Ionic liquid (hereafter denoted as IL) has attracted much attention as a medium that can replace volatile and hazardous organic solvents.[1–17] Chemical properties such as hydrophilicity/hydrophobicity and viscosity can be tuned by designing the structures of component anions and cations, whose properties are of great significance for useful applications to various organic reactions.[1,2,4,18–25] The applications are often influenced by the dynamic aspects of solvation, so that it is desirable to get insight into how reacting species (that is, solute molecules) are dynamically solvated by the component ions in ILs. In this study, we focus on polar water molecule and apolar benzene molecule as representative solutes. Systematically extending the range of solvent ion size and structure, we explore the anion and cation effects on the solute rotational dynamics in view of the intermolecular interaction between neutral solute and ionic solvent.

The rotational dynamics of water and benzene can be elucidated by the rotational correlation time (τ_{2R}) determined by measuring the spin-lattice relaxation time (T_1) of ^{2}H (D) nucleus in ^{2}H NMR spectroscopy. The quadrupolar D nucleus is useful since its relaxation mechanism is directly related to the rotation of the molecule of interest. It should be noted that the solute rotational dynamics is influenced not only by the Coulombic attraction but also by the solvent viscosity. To highlight the effect of Coulombic interaction and compensate the effect of solvent viscosity, we adopt the τ_{2R} ratio of water to benzene, denoted as $\tau_{W/B}$.[26–28] Since benzene is a nonpolar molecule, the parameter $\tau_{W/B}$ reflects the effect of solvent polarity more sensitively than τ_{2R} itself and can be a useful measure of solute-solvent attractive interactions, such as hydrogen bonding and Coulombic attractions. Dependence of the solute dynamics on solute-solvent interaction is examined by varying the anion and cation species composing IL solvent.

In a previous study on the rotational dynamics of water and benzene in 1-butyl-3-methylimidazolium chloride ([$bmim^+$][Cl^-]) and 1-butyl-3-methylimidazolium hexafluorophosphate ([$bmim^+$][PF_6^-]),[26] we showed that the rotation of polar water molecule solvated by a small monoatomic Cl^- anion was significantly slower than that solvated by a larger polyatomic PF_6^- anion. On the other hand, the rotation of apolar benzene molecule was similar in the two ILs. The dynamic contrast between these representative solutes has been interpreted by considering the stronger Coulomb field of the smaller anion as a cause for the slowdown of the rotation of polar water molecule. The concept employed for the interpretation is extensively tested in the present work.

To establish a general role played by Coulombic solute-anion and solute-cation interactions, we employ five [$bmim^+$]-based ILs with anion components of [$HCOO^-$] (formate), [Cl^-], [PF_6^-], [TfO^-] (trifluoromethylsulfonate), and [$TFSI^-$] (bis(trifluoromethylsulfonyl)imide),

a)Author to whom correspondence should be addressed. Electronic mail: nobuyuki@scl.kyoto-u.ac.jp. Tel.: +81-774-38-3071.

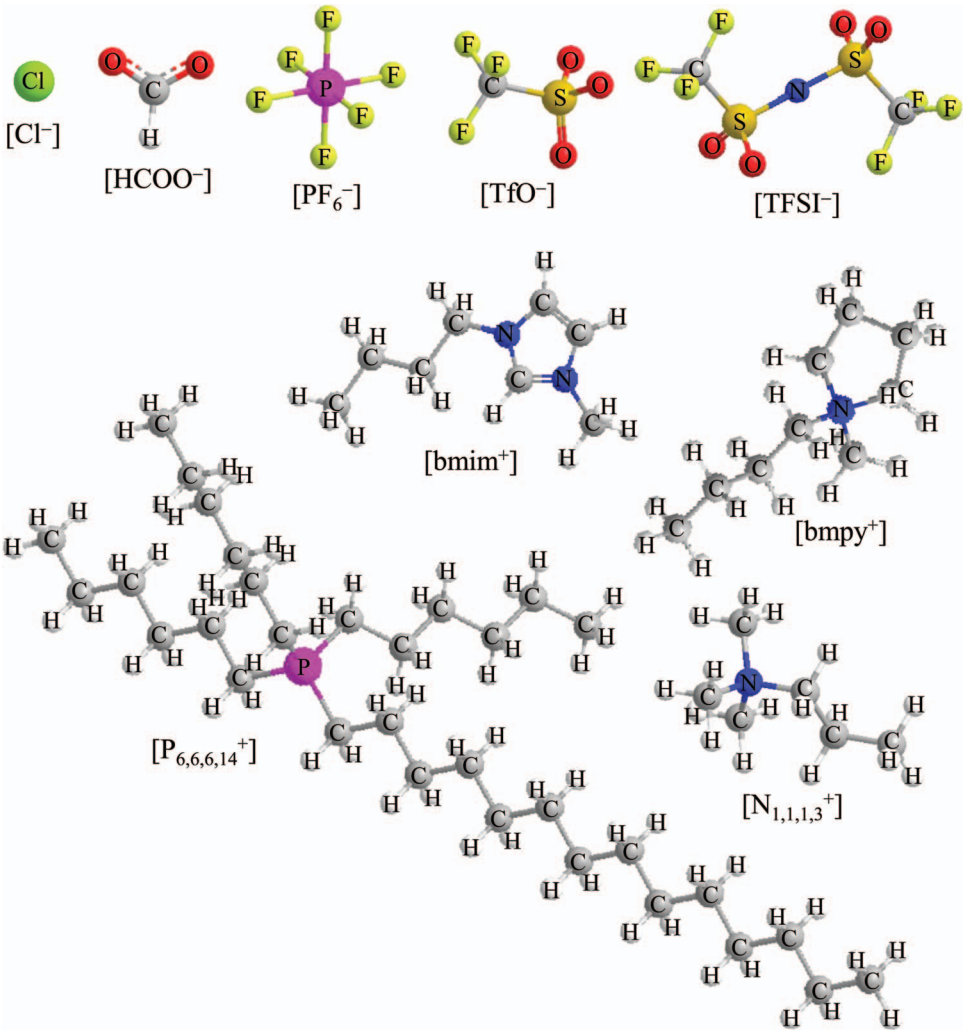

FIG. 1. Structures of the solvent anions and cations.

and four [TFSI$^-$]-based ILs with cation components of [bmim$^+$], [bmpy$^+$] (*N*-methyl-*N*-butylpyrrolidinium), [$N_{1,1,1,3}^+$] (*N*,*N*,*N*-trimethyl-*N*-propylammonium), and [$P_{6,6,6,14}^+$] (*P*,*P*,*P*-trihexyl-*P*-tetradecylphosphonium bis(trifluoromethylsulfonyl)imide); see Fig. 1 for the ion structures. The sizes and chemical structures are markedly different among one another, so that we can effectively comprehend the anion and cation effects on the rotational dynamics of water and benzene.

The NMR spin-lattice relaxation time (T_1) is determined by the Fourier transform of the time correlation function for the relevant rotational motion.[29] The simple Debye mechanism is usually adopted, in which the time correlation function is assumed to decay through the exponential form, $\exp(-t/\tau)$, with τ being the relaxation time. This assumption is problematic in ILs, however. Recent spectroscopic[30–34] and theoretical[35,36] studies have shown that the rotational dynamics in ILs obeys non-exponential functional form. In this study, we analyze the rotational dynamics using a model derived from a previous molecular dynamics (MD) study on the functional form of the time correlation function for the rotational dynamics of water and benzene in IL.[35,36] The long-time tail of the rotational time correlation function was found in Ref. 36 to be the major portion of the spectral density at the NMR Larmor frequency; the slow relaxation is responsible for determining T_1 and is diffusive with exponentially decaying time correlation function. The rotational time correlation function in IL can be thus modeled in a modified Debye form, $A\exp(-t/\tau)$, where the constant A corresponds to the Lipari-Szabo order parameter used in the analysis of protein dynamics.[37,38] We explore in a systematic way how the key parameter τ depends on the solute polarity and the structures of anions and cations in ILs.

II. EXPERIMENTAL

A. Sample preparation

Deuterated water (D_2O, 99.95 at.% D) and benzene (C_6D_6, 99.9 at.% D) were purchased from CEA and used without further purification. 1-Butyl-3-methylimidazolium bis(trifluoromethylsulfonyl)imide ([bmim$^+$][TFSI$^-$]), *N*-methyl-*N*-butylpyrrolidinium bis(trifluoromethylsulfonyl)imide ([bmpy$^+$][TFSI$^-$]), *N*,*N*,*N*-trimethyl-*N*-propylammonium bis(trifluoromethylsulfonyl)imide ([$N_{1,1,1,3}^+$][TFSI$^-$]), and *P*,*P*,*P*-trihexyl-*P*-tetradecylphosphonium bis(trifluoromethylsulfonyl)imide

($[P_{6,6,6,14}^+][TFSI^-]$) were obtained from Kanto Kagaku. These ILs were washed three times with CH_2Cl_2-H_2O mixture (1:1 by volume) and were then extracted to the CH_2Cl_2 phase to remove impurities such as metal ions and acids. The extracts were concentrated and dried using a rotary vacuum pump for 3 days at 80 °C. With the procedure described above, the concentration of impurity water reduced to less than 10^{-3} M (mol dm^{-3}). The impurity water concentration was confirmed by ^{1}H NMR measurement for all of the systems employed in the present study.

1-Butyl-3-methylimidazolium trifluoromethylsulfonate ($[bmim^+][TfO^-]$) was synthesized by metathesis between bis(1-butyl-3-methylimidazolium) sulfate ($[(bmim^+)_2][SO_4^{2-}]$) and strontium trifluoromethylsulfonate ($Sr(TfO)_2$). An aqueous solution of $Sr(TfO)_2$ (1.05 equiv.) was added to a stirred aqueous solution of $[(bmim^+)_2][SO_4^{2-}]$ at room temperature and the resulting mixture was filtered after 30 min. The filtrate was washed three times with CH_2Cl_2-H_2O mixture (2:1 by volume) and was then extracted to the H_2O phase. The extract was concentrated *in vacuo* for 3 days at 80 °C so that the impurity water concentration becomes less than 10^{-2} M.

1-Butyl-3-methylimidazolium formate ($[bmim^+][HCOO^-]$) was synthesized by metathesis between $[(bmim^+)_2][SO_4^{2-}]$ and barium formate ($Ba(HCOO)_2$). Aqueous solutions of $[(bmim^+)_2][SO_4^{2-}]$ and $Ba(HCOO)_2$ (1.05 equiv.) were mixed and stirred for 30 min at room temperature. The mixture was filtered and titrated with $[(bmim^+)_2][SO_4^{2-}]$ solution to remove excess Ba^{2+} down to less than 10^{-3} M, followed by filtration. The concentration of impurity water was then reduced to 5×10^{-3} M by using a rotary vacuum pump for 5 days at a lower temperature of 50 °C; the temperature was 50 °C, instead of 80 °C, because of the low thermal stability of $[bmim^+][HCOO^-]$.

A solute, D_2O or C_6D_6, and a solvent IL were weighed and sealed in a Pyrex NMR tube (5.0 mm o.d.) under nitrogen atmosphere. To remove the possible contribution of the solute-solute interaction, a low concentration of 0.01–0.06 M is adopted. The mixture was heated to reduce the solvent viscosity and was shaken for 10 min to attain complete mixing. The solute concentration was determined by D peak intensity against a D_2O-THF solution (0.05 M) as an external reference.

B. Measurement of spin-lattice relaxation time T_1

The spin-lattice relaxation time (T_1) of ^{2}H (D) was measured at two resonance frequencies of 61.4 MHz (JEOL ECA400W; 9.4 T) and 92.1 MHz (JEOL ECA600; 14.1 T) using the inversion-recovery method with the π-t-$\pi/2$ pulse sequence. In each measurement, the number of delay times t was 30 and the largest t was taken to be more than $10T_1$. The free induction decay signals were accumulated so that the signal-to-noise ratio at the largest t exceeds 10; the scan was done 32–512 times depending on the temperature. The T_1 measurement was conducted when the thermal equilibrium was attained at 1 h after the sample setting. The temperature was controlled within ±1 °C and was calibrated by an alumel-chromel thermocouple using ice water as the reference. The reproducibility of T_1 was within ±1%.

C. T_1 expression in terms of rotational correlation time τ_{2R}

The main relaxation mechanism of D nucleus is the quadrupolar relaxation. The NMR T_1 of D nucleus is related to the second-order rotational time correlation function $C_{2R}(t)$ and its spectral density $j(\omega)$, and is expressed as[29]

$$C_{2R}(t) = \left\langle \frac{3(\vec{n}(t)\cdot\vec{n}(0))^2 - 1}{2} \right\rangle, \tag{1}$$

$$j(\omega) = \mathrm{Re}\int_0^\infty C_{2R}(t)\exp(i\omega t)\mathrm{d}t, \tag{2}$$

$$\frac{1}{T_1} = \frac{3}{10}\pi^2(\mathrm{QCC})^2\{j(\omega) + 4j(2\omega)\}, \tag{3}$$

where ω is the Larmor frequency and $\vec{n}(t)$ is the unit vector of the principle axis of the electric field gradient tensor at the deuterium nucleus at time t. For the D atoms of D_2O and C_6D_6, $\vec{n}$ are essentially the directions of the O−D and C−D bonds, respectively. QCC of Eq. (3) is called quadrupolar coupling constant, and reflects the strength of the interaction between the quadrupole moment of a nucleus and the electric field gradient at the nucleus position. The bracket $\langle\ \rangle$ represents the ensemble average.

When the single exponential form is assumed (Debye model), $C_{2R}(t)$ is given by

$$C_{2R}(t) = \exp(-t/\tau_{2R}). \tag{4}$$

Equation (1) then provides T_1 through

$$\frac{1}{T_1} = \frac{3}{10}\pi^2(\mathrm{QCC})^2\left[\frac{1}{1+(\tau_{2R}\omega)^2} + \frac{4}{1+(2\tau_{2R}\omega)^2}\right]\tau_{2R}. \tag{5}$$

This simple approximation has been commonly adopted in NMR studies.[26,39–43] However, a significant non-exponentiality has been disclosed for $C_{2R}(t)$ in ILs by spectroscopic and MD studies.[30–36] In fact, a long-time MD simulation study[36] showed that $C_{2R}(t)$ is bimodal for water and benzene in a representative IL, $[bmim^+][Cl^-]$; nearly 90% of the correlation is quickly lost within a few ps due to the local dynamics of solute, such as vibration and libration, and then the remaining 10% of the correlation is lost orders-of-magnitude more slowly with relaxation of the solvent structure. The long-time (diffusive) part of $C_{2R}(t)$ was shown to be the time domain relevant to the NMR T_1, with nearly exponential decay in the form of

$$C_{2R}(t) = a\exp(-t/\tau_{2R}), \tag{6}$$

where a expresses the orientational correlation persisting after the short-time (ps-time region) relaxation and is known as Lipari-Szabo factor within the context of protein dynamics.[37,38] Following Eqs. (2), (3), and (6), the NMR T_1

is determined as[36]

$$\frac{1}{T_1} = \frac{3}{10}\pi^2(\mathrm{QCC}^{\mathrm{eff}})^2\left[\frac{1}{1+(\tau_{2\mathrm{R}}\omega)^2} + \frac{4}{1+(2\tau_{2\mathrm{R}}\omega)^2}\right]\tau_{2\mathrm{R}}, \tag{7}$$

where $\mathrm{QCC}^{\mathrm{eff}}$ means the "effective" QCC involving the effect of Lipari-Szabo factor a and is different from the "real" QCC, $\mathrm{QCC}^{\mathrm{real}}$, in Eqs. (3) and (5). As will be shown in Sec. II D, it is not necessary to fix $\mathrm{QCC}^{\mathrm{eff}}$ for determining $\tau_{2\mathrm{R}}$, the rotational correlation time of main interest in the present work. In Appendix A, we discuss the $\mathrm{QCC}^{\mathrm{eff}}$ in detail. In Appendix B, we also discuss the applicability of Eq. (7) in the benzene/IL and water/IL systems.

D. Determination of $\tau_{2\mathrm{R}}$

To determine $\tau_{2\mathrm{R}}$ with Eq. (7), we measured T_1 at the two frequencies using 400 and 600 MHz NMR apparatus; for deuterium, the Larmor frequencies are 61.4 and 92.1 MHz, respectively. When T_1 at the two frequencies (denoted as T_1^{400} and T_1^{600}, respectively) are obtained, we solve Eq. (7) simultaneously and determine $\tau_{2\mathrm{R}}$ through

$$\frac{T_1^{600}}{T_1^{400}} = \frac{\dfrac{1}{1+\left(\tau_{2\mathrm{R}}\omega_0^{400}\right)^2} + \dfrac{4}{1+\left(2\tau_{2\mathrm{R}}\omega_0^{400}\right)^2}}{\dfrac{1}{1+\left(\tau_{2\mathrm{R}}\omega_0^{600}\right)^2} + \dfrac{4}{1+\left(2\tau_{2\mathrm{R}}\omega_0^{600}\right)^2}}, \tag{8}$$

where ω_0^{400} and ω_0^{600} are the relevant deuterium Larmor angular frequencies. Note that the $\mathrm{QCC}^{\mathrm{eff}}$ is eliminated by the division. In principle, $\tau_{2\mathrm{R}}$ can be numerically determined at any condition through Eq. (8); the reliability of Eq. (8) in analyzing the NMR T_1 is demonstrated in Appendix B. The numerical procedure can be processed with good precision in practice, however, only when the T_1 difference at the two resonance frequencies is sufficiently large (>10%) compared to the errors in measured T_1 (~1%). As is seen in Fig. 2, for example, the difference between T_1^{400} and T_1^{600} for benzene in [bmim$^+$][TFSI$^-$] is large enough when $\tau_{2\mathrm{R}}$ is ~500 ps or larger. A larger $\tau_{2\mathrm{R}}$ corresponds to a slower relaxation of the rotational motion. Accordingly, T_1^{400} and T_1^{600} are desirable to be measured at low enough temperatures to slow the rotation.

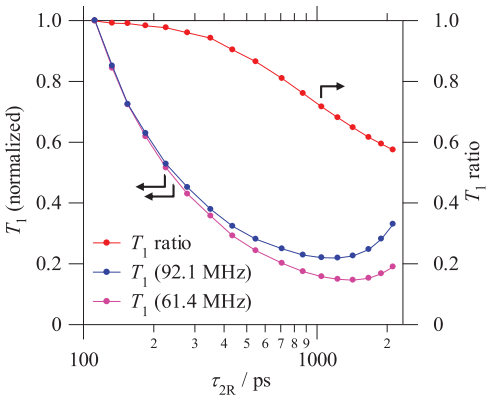

FIG. 2. $\tau_{2\mathrm{R}}$ dependence of T_1 at the two resonance frequencies of $\omega_0 = 61.4$ and 92.1 MHz, and their ratio. The T_1 value is normalized to the value at $\tau_{2\mathrm{R}} = 120$ ps and $\omega_0 = 92.1$ MHz.

III. RESULTS AND DISCUSSION

The time constant $\tau_{2\mathrm{R}}$ determined experimentally through Eq. (8) characterizes the rotational relaxation in the diffusive tail. When the effect of such specific interaction as hydrogen bonding is weak in the time region of interest,[44] the Stokes-Einstein-Debye (SED) law holds and $\tau_{2\mathrm{R}}$ is expressed as

$$\tau_{2\mathrm{R}} = \frac{V_m}{k_{\mathrm{B}}}\frac{\eta}{T}, \tag{9}$$

TABLE I. Experimental conditions for the T_1 measurements and the $\mathrm{QCC}^{\mathrm{eff}}$ in the ILs.

Solvent	Solute	c (M)[a]	T_{mes} (°C)[b]	T_{QCC} (°C)[c]	$\mathrm{QCC}^{\mathrm{eff}}$ (kHz)[d]
[bmim$^+$][HCOO$^-$]	D_2O	0.06	30 – 80	30, 35, 40	140 ± 1
	C_6D_6	0.04	10 – 80	10, 20	67 ± 1
[bmim$^+$][TfO$^-$]	D_2O	0.05	− 10 – 80	−10, −5, 0	132 ± 4
	C_6D_6	0.03	0 – 80	0, 5, 10	66 ± 1
[bmim$^+$][Cl$^-$][e]	D_2O	0.05	60 – 100	60, 65, 70	144 ± 2
	C_6D_6	0.02	70 – 100	70, 75, 80	60 ± 2
[bmim$^+$][PF_6^-][e]	D_2O	0.05	5 – 70	5, 10, 15	89 ± 5
	C_6D_6	0.02	25 – 100	25, 30, 35	64 ± 2
[bmim$^+$][TFSI$^-$]	D_2O	0.03	− 30 – 80	−30, −25, −20	120 ± 5
	C_6D_6	0.03	− 10 – 80	−10, −5, 0	68 ± 1
[bmpy$^+$][TFSI$^-$]	D_2O	0.06	− 20 – 80	−20, −15, −10	119 ± 4
	C_6D_6	0.01	− 10 – 80	−10, 0, 10	68 ± 1
[$N_{1,1,1,3}^+$][TFSI$^-$]	D_2O	0.04	− 30 – 80	−30, −25, −20	120 ± 5
	C_6D_6	0.01	− 10 – 80	0, 5, 10	68 ± 1
[$P_{6,6,6,14}^+$][TFSI$^-$]	D_2O	0.03	0 – 80	0, 5, 10	81 ± 2
	C_6D_6	0.03	5 – 80	5, 10, 15	57 ± 1

[a]The molar concentration of the solute.
[b]The temperature range where the T_1 measurements were carried out.
[c]The temperature at which the $\mathrm{QCC}^{\mathrm{eff}}$ was determined.
[d]The $\mathrm{QCC}^{\mathrm{eff}}$ is different from the real QCC, $\mathrm{QCC}^{\mathrm{real}}$, in Eqs. (3) and (5) and is introduced as $\mathrm{QCC}^{\mathrm{eff}} = \sqrt{A}\,\mathrm{QCC}^{\mathrm{real}}$ in Eq. (A4); see the text. The $\mathrm{QCC}^{\mathrm{eff}}$ value was averaged over the temperatures listed as T_{QCC}.
[e]Reference 26.

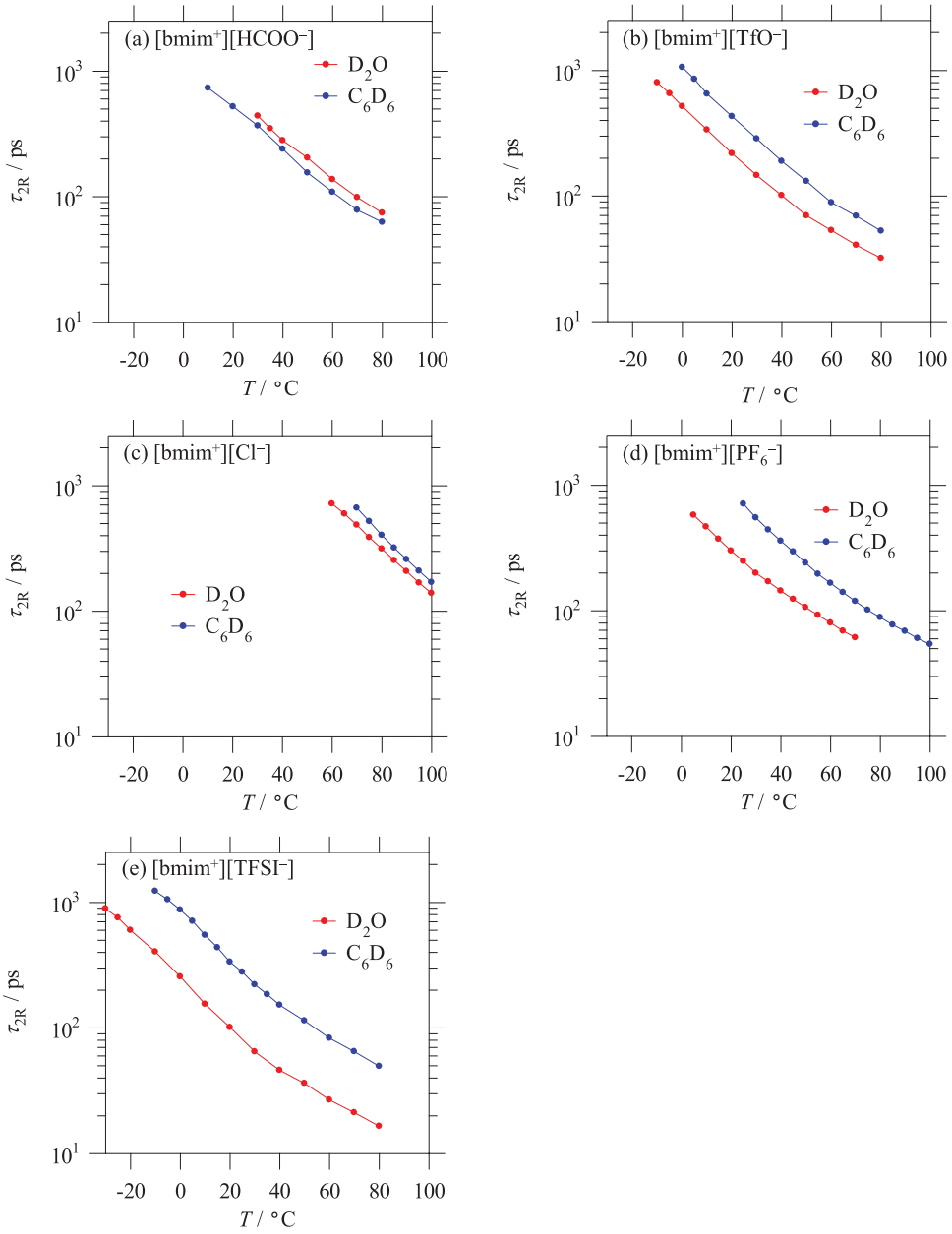

FIG. 3. Temperature dependence of τ_{2R} for D_2O and C_6D_6 in the [bmim$^+$]-based ILs composed with (a) [HCOO$^-$], (b) [TfO$^-$], (c) [Cl$^-$], (d) [PF$_6^-$], and (e) [TFSI$^-$]. For both solutes, τ_{2R} increases with decreasing temperature (increasing the solvent viscosity).

where k_B is the Boltzmann constant, V_m is the spherically averaged effective hydrodynamic volume of the solute molecule, and η and T are the solvent viscosity and the temperature, respectively. When we take the ratio, $\tau_{W/B}$, of τ_{2R} of water to benzene, we have

$$\tau_{W/B} = \frac{\tau_{2R,W}}{\tau_{2R,B}} = \frac{V_{m,W}}{V_{m,B}}. \quad (10)$$

The effect of the solvent viscosity is cancelled, and $\tau_{W/B}$ is equal to the hydrodynamic volume ratio of water to benzene, $V_{m,W}/V_{m,B}$, which was determined to be 1/15 according to the SED law applied to an apolar organic solvent, carbon tetrachloride (CCl_4).[27,28] In ILs with Coulombic interaction involving a full charge of the solvent ion, however, we will see that the SED law is invalid and that the actual $\tau_{W/B}$ value deviates from 1/15 predicted by the SED law. This deviation can be a measure of Coulombic interaction, in view of the fact that polar water is subject to a stronger Coulombic interaction compared with apolar benzene. We will use $\tau_{W/B}$ to quantitatively probe the Coulombic solute-solvent interaction in ILs and elucidate the anion and cation effects on the solute dynamics.

A. Anion effect

First we show how the anion size and structure affect the solute dynamics by comparing the τ_{2R} values for water and benzene in [bmim$^+$]-based ILs with anion components of [TFSI$^-$], [TfO$^-$], [PF$_6^-$], [Cl$^-$], and [HCOO$^-$]. The anion

TABLE II. τ_{2R} of water and benzene and their ratio, $\tau_{W/B}$, at 70 °C.[a]

Solvent	τ_{2R} (ps) D_2O	τ_{2R} (ps) C_6D_6	$\tau_{W/B}$
[bmim$^+$][Cl$^-$]	486	663	0.73
[bmim$^+$][HCOO$^-$]	98.6	78.3	1.25
[bmim$^+$][PF$_6^-$][b]	61.2	119	0.52
[bmim$^+$][TfO$^-$][b]	40.6	69.4	0.58
[bmim$^+$][TFSI$^-$]	21.2	65.0	0.32
[bmpy$^+$][TFSI$^-$]	26.4	91.8	0.29
[$N_{1,1,1,3}^+$][TFSI$^-$]	21.8	86.0	0.27
[$P_{6,6,6,14}^+$][TFSI$^-$]	224	167	1.34
CH_3CN (50 °C)	0.475[c]	0.95[d]	0.50
C_6H_6 (50 °C)	0.183[c]	1.03[d]	0.18
CCl_4 (40 °C)	0.826[c]	1.28[d]	0.06

[a]The $\tau_{W/B}$ values determined at the different temperatures (T_{mes} in Table I) agree within ~4%, except for [$P_{6,6,6,14}^+$][TFSI$^-$]; see Sec. III B.
[b]Reference 26.
[c]Reference 27.
[d]Reference 28.

size sequence is[45,46]

$$\mathrm{Cl}^-(1.8\,\text{Å}) < \mathrm{HCOO}^-(1.8-1.9\,\text{Å}) < \mathrm{PF}_6^-(2.6\,\text{Å}) < \mathrm{TfO}^-(2.7\,\text{Å}) < \mathrm{TFSI}^-(3.3\,\text{Å}), \quad (11)$$

where the numbers in parentheses show the radii of the anions. The experimental conditions for the T_1 measurement to determine τ_{2R} and QCC^{eff} through Eqs. (7) and (8) are summarized in Table I.

1. τ_{2R} for water and benzene

In Fig. 3, we show τ_{2R} for water and benzene in the [bmim$^+$]-based ILs as a function of temperature.[26] Except for [bmim$^+$][HCOO$^-$], τ_{2R} is larger for benzene than for water over the temperature range examined. This is primarily because the rotation of benzene is hampered more strongly due to the larger volume by a factor of 15 (SED law).[27,28] However, the τ_{2R} ratio ($\tau_{W/B}$) deviates from the volume ratio due to the effect of Coulombic interaction, as will be discussed in Sec. III A 2. In the ILs with smaller anions which has higher charge density and stronger Coulombic attraction, the rotation of water is retarded more strongly and τ_{2R} for water tends to be closer to that for benzene. In [bmim$^+$][HCOO$^-$], in particular, τ_{2R} is larger for water than for benzene despite the smaller volume. To elucidate the effect of Coulombic solute-solvent interaction, we take $\tau_{W/B}$ defined by Eq. (10), the τ_{2R} ratio of water to benzene.

2. τ_{2R} ratio of water to benzene

The $\tau_{W/B}$ value in each IL is listed in Table II and is plotted against the anion size in Fig. 4. A general trend is that $\tau_{W/B}$ is larger for smaller anion. According to the definition of $\tau_{W/B}$ in Eq. (10), $\tau_{W/B}$ reflects the effect of Coulombic solute-solvent attraction more dominantly than τ_{2R} itself, so that we can regard $\tau_{W/B}$ as a measure of hydrophilicity of IL. $\tau_{W/B}$ is also convenient to discuss the solvent effect without taking into account the temperature effect. The $\tau_{W/B}$ values

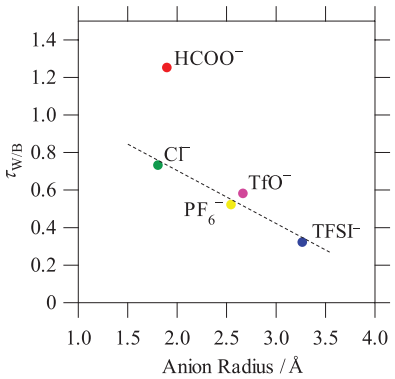

FIG. 4. Correlation of $\tau_{W/B}$ in the [bmim$^+$]-based ILs with the anion radius.

agree within ~4% among the temperatures examined and are essentially independent of temperature.

In [bmim$^+$][TFSI$^-$], the largest and most hydrophobic anion employed in this study, $\tau_{W/B}$ is 0.32 and is smaller than in the other ILs. Compared with the $\tau_{W/B}$ values in organic solvents previously studied,[26] $\tau_{W/B}$ is larger in [bmim$^+$][TFSI$^-$] than in nonpolar C_6H_6 and tetrachloromethane (CCl_4), but is smaller than in polar acetonitrile (CH_3CN). This means that the water dynamics is slowed down by the Coulomb attraction more strongly in CH_3CN than in [bmim$^+$][TFSI$^-$]. In CH_3CN, water can form a hydrogen bond with the negatively charged N ($N^{\delta-} \equiv C^{\delta+}$) atom of the solvent molecule.[27,28] In [bmim$^+$][TFSI$^-$], water is solvated by TFSI$^-$ anion and/or bmim$^+$ cation. Although TFSI$^-$ anion is fully negatively charged, the negative charge is distributed over the electronegative O and F atoms. This can account for a weaker Coulomb attraction in [bmim$^+$][TFSI$^-$] than in CH_3CN.

Although the size of TfO$^-$ is larger than of PF_6^- (see Eq. (11)), $\tau_{W/B}$ is smaller in [bmim$^+$][TfO$^-$] than in [bmim$^+$][PF_6^-]; see Table II. This is due to the difference in the atomic partial charges; the partial charges of the sulfonyl O atoms of TfO$^-$ and the F atoms of PF_6^- are −0.63 and −0.39, respectively.[47] The Coulombic water-anion interaction is larger in [bmim$^+$][TfO$^-$] than in [bmim$^+$][PF_6^-] due to the stronger hydrogen bond formation with the more negatively charged O atoms of TfO$^-$ compared with the F atoms of PF_6^-. The $\tau_{W/B}$ values for these two ILs are slightly larger than for CH_3CN, and the strength of the attractive interactions with these anions is almost equal to that of the hydrogen bonds with CH_3CN molecules.

In the case of [bmim$^+$][HCOO$^-$], $\tau_{W/B}$ is 1.25 and is by far larger than that for the hydrophilic [bmim$^+$][Cl$^-$]; see Table II. This is attributed to the double hydrogen-bonding formation between one D atom of the water molecule and the carbonyl O of the HCOO$^-$ anion and between the other D atom of water and the carboxyl O of HCOO$^-$. The carbonyl and carboxyl O atoms of the HCOO$^-$ anion are conjugate, and the water motion can be slowed down by the formation of the two hydrogen bonds.

B. Cation effect

The imidazolium cation has an aromatic ring. Thus, the following questions arise. (i) Is the dynamics for benzene

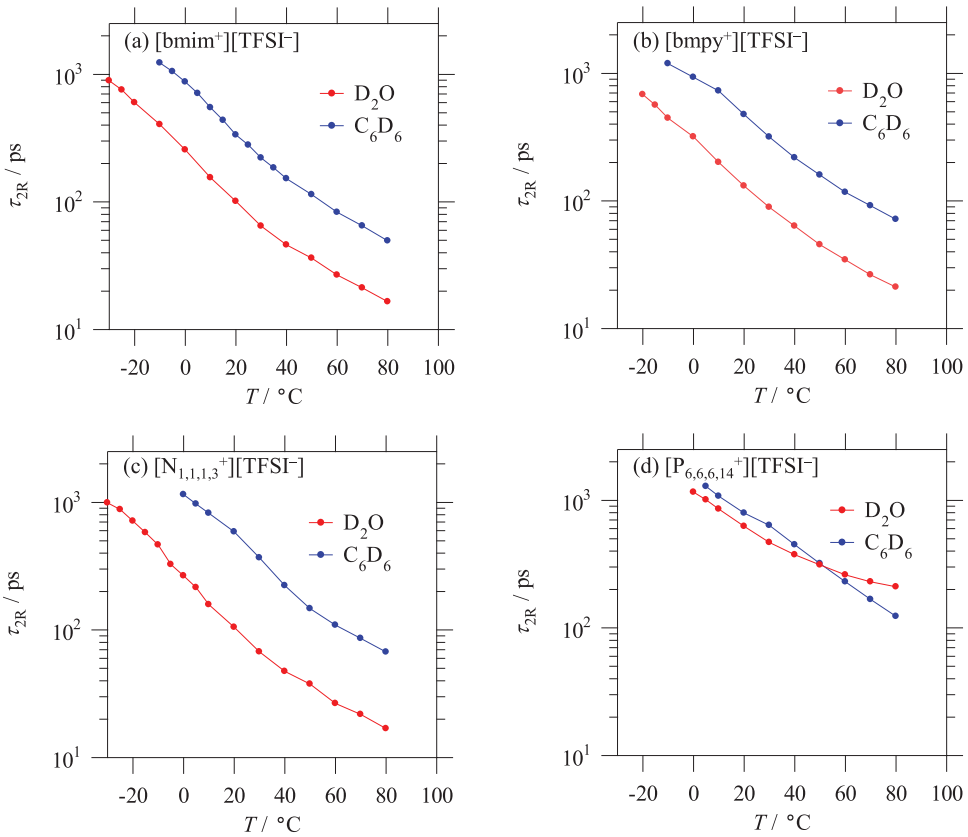

FIG. 5. Temperature dependence of τ_{2R} for D_2O and C_6D_6 in the [$TFSI^-$]-based ILs composed with (a) [$bmim^+$], (b) [$bmpy^+$], (c) [$N_{1,1,1,3}{}^+$], and (d) [$P_{6,6,6,14}{}^+$].

affected by the imidazolium cation via its aromatic ring (π-π interaction)? A MD simulation of benzene in [$mmim^+$][$PF_6{}^-$] by Lynden-Bell *et al.* showed that the aromatic ring of the imidazolium cation interacts with the benzene ring.[48] (ii) Does the charge density of cation affect the solute dynamics as in the case of anion? (iii) How is the shielding effect of the bulky alkyl chains? In view of these, we investigate the solute dynamics in alkylammonium, pyrrolidinium, and phosphonium cations, in which the positive charge is localized on the N and P atoms and screened against the solute molecule by the bulky alkyl chains. The experimental conditions are summarized in Table I.

Let us see how the rotational dynamics of water and benzene vary with the cation. Figure 5 shows the τ_{2R} values for water and benzene in the [$TFSI^-$]-based ILs with cation components of (a) [$bmim^+$], (b) [$bmpy^+$], (c) [$N_{1,1,1,3}{}^+$], and (d) [$P_{6,6,6,14}{}^+$] as a function of temperature. When Figs. 5(a)–5(c) are compared, it is found for both water and benzene that τ_{2R} does not exhibit strong dependence on the cation species. When attention is paid to $\tau_{W/B}$, the values in the ILs agree among one another within ~10%; see Table II. These clearly indicate that the π-π interaction, the charge distribution, and the charge screening are all of insignificance for the solute rotational dynamics. In the largest and most hydrophobic [$P_{6,6,6,14}{}^+$][$TFSI^-$], as shown in Fig. 5(d), a different tendency is observed. Water has a larger τ_{2R} than does benzene at high temperatures (>50 °C). This seems to suggest a unique solvation structure in the [$P_{6,6,6,14}{}^+$]-based ILs. The hydrophobic bulky alkyl chains on the phosphonium cation dispel polar water molecule, in particular, so that water molecules can be preferably close to the component anions, leading to the remarkable slowdown of the rotation. Because of the crossover of τ_{2R} between water and benzene, $\tau_{W/B}$ fluctuates significantly against the temperature. In such a case, $\tau_{W/B}$ cannot be a good probe to characterize the solute-solvent attractive interaction.

IV. CONCLUSIONS

In order to comparatively investigate the rotational dynamics of polar water (D_2O) and apolar benzene (C_6D_6) molecules in ILs, we determined the rotational correlation time (τ_{2R}) by means of the ^2H (D) NMR spin-lattice relaxation time T_1 measurement. To elucidate the anion effect on the solute rotational dynamics, we studied five [$bmim^+$]-based ILs with anion components of [$TFSI^-$], [TfO^-], [$PF_6{}^-$], [Cl^-], and [$HCOO^-$]. To examine the cation effect, we compared four [$TFSI^-$]-based ILs with cation components of [$bmim^+$], [$bmpy^+$], [$N_{1,1,1,3}{}^+$], and [$P_{6,6,6,14}{}^+$].

We employed the τ_{2R} ratio of water to benzene, denoted as $\tau_{W/B}$, to highlight the effect of Coulombic attraction by solvent ions on the solute rotational dynamics. Although $\tau_{W/B}$ is estimated as 1/15 according to the Stokes-Einstein-Debye law, it is actually ~0.3 and more when Coulombic solute-solvent attractive interaction is strongly operative. A general tendency is that $\tau_{W/B}$ is larger for smaller anion. When the

anion size is as large as $TFSI^-$, the strength of Coulombic attraction characterized by $\tau_{W/B}$ is weaker than in polar organic solvent, acetonitrile. The $HCOO^-$ is notable in that its ability of bidentate coordination leads to the largest $\tau_{W/B}$ irrespective of the anion size. For both water and benzene solutes, τ_{2R} is strongly dependent on the temperature, corresponding to the reduction of solvent viscosity with the temperature. For the parameter $\tau_{W/B}$, though, the temperature effect is canceled and its value is almost independent of the temperature. In contrast to the anion effect, $\tau_{W/B}$ does not exhibit strong dependence on the cation species. Only the largest and most hydrophobic $P_{6,6,6,14}{}^+$ cation gives an exceptionally large $\tau_{W/B}$. This indicates a unique solvation structure of water and/or benzene in [$P_{6,6,6,14}{}^+$]-based ILs.

ACKNOWLEDGMENTS

This work is supported by the Grants-in-Aid for Scientific Research (Grant Nos. 21300111 and 23651202) from the Japan Society for the Promotion of Science, by the Grant-in-Aid for Scientific Research on Innovative Areas (Grant No. 20118002) and the Elements Strategy Initiative for Catalysts & Batteries from the Ministry of Education, Culture, Sports, Science, and Technology, and by the Nanoscience Program, the Computational Materials Science Initiative, and the Strategic Programs for Innovative Research of the Next-Generation Supercomputing Project. M.N. acknowledges the support for the Water Chemistry Energy Laboratory from Asahi Glass Co., Ltd.

APPENDIX A: DETERMINATION OF EFFECTIVE QUADRUPOLAR COUPLING CONSTANT (QCC^{eff})

The rotational time correlation function $C_{2R}(t)$ in IL is not of a simple exponential form given by Eq. (4), as mentioned in Sec. II C. According to a MD simulation study,[36] $C_{2R}(t)$ (renamed as $C_{2R}^{total}(t)$ hereafter) can be divided into two components, $C_{2R}^{fast}(t)$ and $C_{2R}^{diff}(t)$, expressed as

$$\begin{cases} C_{2R}^{diff}(t) = a\exp(-t/\tau_{2R}) \\ C_{2R}^{fast}(t) = C_{2R}^{total}(t) - C_{2R}^{diff}(t) \end{cases}, \tag{A1}$$

where $C_{2R}^{diff}(t)$ is the diffusive tail of $C_{2R}^{total}(t)$ extrapolated to time 0 and $C_{2R}^{fast}(t)$ is the difference between $C_{2R}^{total}(t)$ and $C_{2R}^{diff}(t)$. The constant a contains the integrated contribution of the short-time relaxation and corresponds to the Lipari-Szabo factor used in the analysis of protein dynamics.[37,38] This decomposition leads to the following expression for spectral density:

$$j^{total}(\omega) = j^{fast}(\omega) + j^{diff}(\omega) = \left\{1 + \frac{\alpha(\omega)}{1-\alpha(\omega)}\right\} j^{diff}(\omega)$$
$$= \frac{a}{1-\alpha(\omega)} \times \frac{\tau_{2R}}{1+(\omega\tau_{2R})^2}, \tag{A2}$$

where

$$\alpha(\omega) = \frac{j^{fast}(\omega)}{j^{total}(\omega)} \tag{A3}$$

and is a correction from the fast part ($C_{2R}^{fast}(t)$) of the rotational time correlation function. As for the frequency dependence of $\alpha(\omega)$, we will see in Appendix B that $\alpha(\omega) = \alpha(2\omega) \equiv \alpha$ can be safely assumed. By substituting Eq. (A2) into Eq. (3), one obtains

$$\frac{1}{T_1} = \frac{3}{10}\pi^2(\sqrt{A}QCC)^2\left[\frac{1}{1+(\tau_{2R}\omega)^2} + \frac{4}{1+(2\tau_{2R}\omega)^2}\right]\tau_{2R}, \tag{A4}$$

where

$$A = \frac{a}{1-\alpha} \tag{A5}$$

and QCC is a quadrupolar coupling constant introduced in Eq. (3). Note the similarity of Eqs. (5) and (A4). Equation (A4) is obtained by replacing the QCC in Eq. (5) with the one multiplied by $\sqrt{A}$. Since A in Eqs. (A4) and (A5) cannot be fixed in the present T_1 measurement, the value of QCC cannot be determined in the present work. Instead, we determine the "effective" QCC (QCC^{eff}), which is the "real" QCC (QCC^{real}) multiplied by the square root of A, i.e., $QCC^{eff} = \sqrt{A}QCC^{real}$ and appears in Eq. (7); see Table I. The QCC^{eff} values are between ~50 and ~140 kHz and are significantly smaller than the QCC^{real} values typically obtained for C−D and O−D deuterons.[49–51]

According to Eq. (A4), the solvent dependence of the QCC^{eff} may contain both the solvent effects on A and QCC^{real}. In our previous MD study,[36] α was found to be up to ~0.4. As shown in Eqs. (A4), the NMR T_1 is governed by $\sqrt{A}$ instead of A itself. The observation of $\alpha < \sim 0.4$ then shows that $\sqrt{A}$ is close to $\sqrt{a}$, and A is also considered to represent the correlation that persists after the initial relaxation and is larger when the initial relaxation decay of correlation is less significant.

In a MD simulation study,[36] we showed that $C_{2R}^{total}(t)$ for benzene in [$bmim^+$][Cl^-] decays to 0.1 (90% relaxation) in the ps-time region. The initial relaxation is dominantly given by the (caged) local dynamics of solute (vibration and libration) and the benzene C−H bond is considered not to be involved in a strong hydrogen bonding with any anions and cations. It is thus assumed that the anion and cation effects on A are relatively small and that the A values are almost identical for all the IL solvents studied. In view of this, we can roughly estimate the QCC^{real} of benzene by multiplying the QCC^{eff} in Table I by $1/\sqrt{0.1}$ (~3). The estimated QCC^{real} is in the range of 170−200 kHz for the ILs studied and coincides with the QCC^{real} value known for pure liquid benzene (193 kHz).[50] This is reasonable, given that benzene is nonpolar and less affected by the Coulombic field in the ILs.

In the case of polar water, the QCC^{eff} obtained is larger for the hydrophilic (large $\tau_{W/B}$) ILs, and is smaller for the hydrophobic (small $\tau_{W/B}$), in correspondence to the strength of hydrogen bond interaction. We attribute the solvent effect on the QCC^{eff} primarily to the change of A with the solvent for the following reason. When a water molecule is involved in strong Coulombic interaction with the solvent ions in hydrophilic IL, it is expected that the local librational motion of water molecule is hampered. This may cause a slowdown of the initial relaxation of the O−D bond reorientation. Thus, the constant A (almost equal to the correlation persisting after

the initial relaxation) should be larger (less initial decay) for hydrophilic IL.

To estimate A, let us suppose that the QCC^{real} for water in the ILs is between the pure liquid (256 kHz) and the ice values (213 kHz).[51] With $QCC^{real} = 256$ kHz and QCC^{eff} in Table I, A is estimated as ∼0.3 in the hydrophilic [bmim$^+$][HCOO$^-$] and is between ∼0.1 and ∼0.2 in the hydrophobic ILs. With $QCC^{real} = 213$ kHz, A is ∼0.4 in [bmim$^+$][HCOO$^-$] and is again between ∼0.1 and ∼0.2 in the hydrophobic ILs. In any case, A tends to be larger in hydrophilic ILs than in hydrophobic. This is a support of the dynamical picture for the O−D reorientation described above.

APPENDIX B: FREQUENCY DEPENDENCE OF CORRECTION FACTOR $\alpha(\omega)$ IN EQ. (A2) AND ITS EFFECT ON SOLUTE ROTATIONAL DYNAMICS

The rotational correlation time (τ_{2R}) for water and benzene were determined from the spin-lattice relaxation time (T_1^{400} and T_1^{600}) measurements at two Larmor frequencies (using 400 and 600 MHz NMR machines, respectively) through Eq. (8), as described in Sec. II D. Note that Eq. (8) is obtained from Eqs. (3) and (A2) under the assumption that the correction factor $\alpha(\omega)$ in Eq. (A2) is independent of the frequency (say, $\alpha(\omega) = \alpha(2\omega)$). In a previous MD study, we found that $\alpha(\omega)$ does not vary with the frequency except at low temperatures near the melting point, around which T_1 takes a minimum. In the present study, temperatures close to this range were adopted for the NMR T_1 measurement in order that the difference between T_1^{400} and T_1^{600} is large enough (>10%) to numerically determine τ_{2R} with good precision. A danger is then that the assumption of $\alpha(\omega) = \alpha(2\omega)$ may not be valid. In order to see the reliability of Eq. (8), therefore, the frequency dependence of $\alpha(\omega)$ and its effect on τ_{2R} need to be examined. In the following, the ^{1}H NMR frequency f in MHz is adopted as the argument of the correction factor α, rather than the radial frequency ω in rad s^{-1}. This convention is employed even in the treatment of ^{2}H (D) since a NMR apparatus is usually termed, for example, with 400 MHz or 600 MHz (for ^{1}H frequency). For example, $\alpha(f)$ obtained at

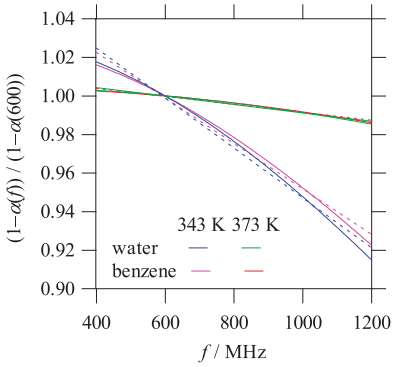

FIG. 6. Plots of $(1 - \alpha(f))/(1 - \alpha(600))$ for water and benzene in [bmim$^+$][Cl$^-$] against the ^{1}H NMR frequency f. The solid lines are taken from the MD simulation results in Ref. 36. The dashed lines are the linear fits. According to the slope, the k value is 0.08 (343 K), and 0.01 (373 K) for water, and 0.07 (343 K), and 0.01 (373 K) for benzene. Note that the water and benzene data are hardly distinguishable from each other within the resolution of the figure.

400 and 600 MHz for ^{1}H nucleus (corresponding to 61.4 and 92.1 MHz for ^{2}H nucleus, respectively) are denoted $\alpha(400)$ and $\alpha(600)$, respectively.

Equations (3) and (A2) provide $1/T_1^{400}$ and $1/T_1^{600}$, respectively, as

$$\frac{1}{T_1^{400}} = \frac{3}{10}\pi^2(\sqrt{a}\mathrm{QCC})^2\left[\frac{1}{1-\alpha(400)} \times \frac{1}{1+\left(\tau_{2R}\omega_0^{400}\right)^2} + \frac{1}{1-\alpha(800)} \times \frac{4}{1+\left(2\tau_{2R}\omega_0^{400}\right)^2}\right]\tau_{2R}, \quad \text{(B1)}$$

$$\frac{1}{T_1^{600}} = \frac{3}{10}\pi^2(\sqrt{a}\mathrm{QCC})^2\left[\frac{1}{1-\alpha(600)} \times \frac{1}{1+\left(\tau_{2R}\omega_0^{600}\right)^2} + \frac{1}{1-\alpha(1200)} \times \frac{4}{1+\left(2\tau_{2R}\omega_0^{600}\right)^2}\right]\tau_{2R}. \quad \text{(B2)}$$

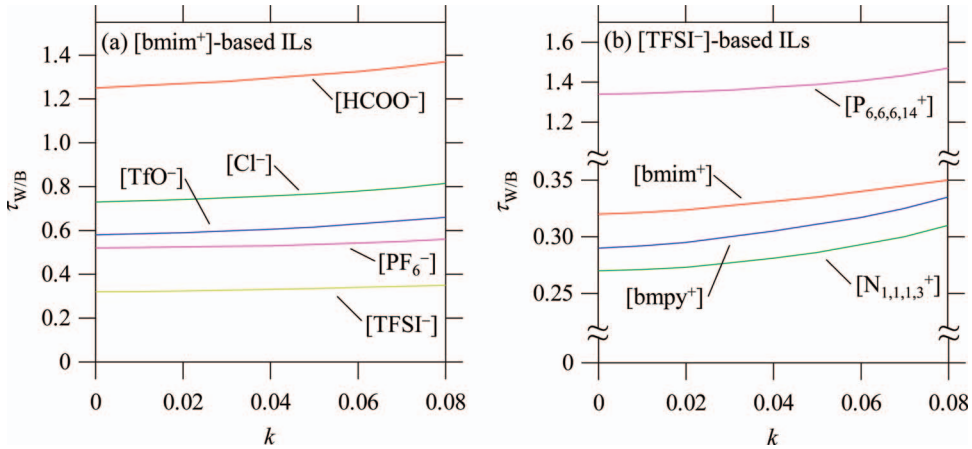

FIG. 7. Plots of $\tau_{W/B}$ at 70 °C against k ($0 \le k \le 0.08$): (a) [bmim$^+$]-based ILs composed with [HCOO$^-$] (red), [TfO$^-$] (blue), [Cl$^-$] (green), [PF$_6^-$] (pink), and [TFSI$^-$] (yellow) and (b) [TFSI$^-$]-based ILs composed with [bmim$^+$] (red), [bmpy$^+$] (blue), [N$_{1,1,1,3}^+$] (green), and [P$_{6,6,6,14}^+$] (pink). The values of $\tau_{W/B}$ for each IL show at most ∼10% increment with increasing k.

By taking their ratio, we obtain

$$\frac{T_1^{600}}{T_1^{400}} = \frac{\frac{1-\alpha(600)}{1-\alpha(400)} \times \frac{1}{1+(\tau_{2R}\omega_0^{400})^2} + \frac{1-\alpha(600)}{1-\alpha(800)} \times \frac{4}{1+(2\tau_{2R}\omega_0^{400})^2}}{\frac{1}{1+(\tau_{2R}\omega_0^{600})^2} + \frac{1-\alpha(600)}{1-\alpha(1200)} \times \frac{4}{1+(2\tau_{2R}\omega_0^{600})^2}}. \tag{B3}$$

Note that the terms containing $\alpha(f)$ are not eliminated by division: cf., Eq. (8). We analyze Eq. (B3) using a linear approximation of

$$\frac{1-\alpha(f)}{1-\alpha(600)} = 1 - k\left(\frac{f}{600} - 1\right), \tag{B4}$$

where k is a constant. Equation (B4) is validated in Fig. 6; the figure shows the f dependence of the left-hand side of Eq. (B4) for [bmim$^+$][Cl$^-$] system treated in Ref. 36. k of Eq. (B4) is dimensionless, and its values for both water and benzene are seen to be within the range of 0−0.08 and be almost identical to each other at temperatures down to the melting point of the IL. For all the cases of ILs studied here, the T_1 measurements were performed near the melting temperatures or higher. The k values for water and benzene in the ILs are then expected to be in the range of 0−0.08 and be coincident to each other. By substituting Eq. (B4) into the right-hand side of Eq. (B3), we obtain

$$\frac{T_1^{600}}{T_1^{400}} = \frac{\frac{1}{1+\frac{1}{3}k} \times \frac{1}{1+(\tau_{2R}\omega_0^{400})^2} + \frac{1}{1-\frac{1}{3}k} \times \frac{4}{1+(2\tau_{2R}\omega_0^{400})^2}}{\frac{1}{1+(\tau_{2R}\omega_0^{600})^2} + \frac{1}{1-k} \times \frac{4}{1+(2\tau_{2R}\omega_0^{600})^2}}. \tag{B5}$$

We redetermined τ_{2R} for water and benzene in each IL from Eq. (B5), assuming that k is in the range of $0 \le k \le 0.08$ and is common between water and benzene. It is found that τ_{2R} for water and benzene may change by a factor of ∼1.3 and ∼1.2, respectively, as k increases from 0 to 0.08. Correspondingly, as illustrated in Fig. 7, the τ_{2R} ratios ($\tau_{W/B}$) of water to benzene for the ILs show at most ∼10% variation compared to those listed in Table II. The ranking of $\tau_{W/B}$ for the ILs does not change from that shown in Table II, showing whether or not $\alpha(f)$ depends on the frequency is insignificant in the present treatment.

[1] T. Welton, Chem. Rev. **99**, 2071 (1999).
[2] J. Dupont, R. F. de Souza, and P. A. Z. Suarez, Chem. Rev. **102**, 3667 (2002).
[3] M. Smiglak, A. Metlen, and R. D. Rogers, Acc. Chem. Res. **40**, 1182 (2007).
[4] P. Hapiot and C. Lagrost, Chem. Rev. **108**, 2238 (2008).
[5] N. V. Plechkova and K. R. Seddon, Chem. Soc. Rev. **37**, 123 (2008).
[6] M. J. Earle, J. M. S. S. Esperanca, M. A. Gilea, J. N. C. Lopes, L. P. N. Rebelo, J. W. Magee, K. R. Seddon, and J. A. Widegren, Nature (London) **439**, 831 (2006).
[7] J. N. A. C. Lopes and A. A. H. Pádua, J. Phys. Chem. B **110**, 3330 (2006).
[8] J. N. C. Lopes and A. A. H. Pádua, J. Phys. Chem. B **110**, 19586 (2006).
[9] T. Köddermann, C. Wertz, A. Heintz, and R. Ludwig, Angew. Chem., Int. Ed. **45**, 3697 (2006).
[10] T. Köddermann, D. Paschek, and R. Ludwig, ChemPhysChem **8**, 2464 (2007).
[11] S. H. Chung, R. Lopato, S. G. Greenbaum, H. Shirota, E. W. Castner, Jr., and J. F. Wishart, J. Phys. Chem. B **111**, 4885 (2007).
[12] E. W. Castner, Jr., J. F. Wishart, and H. Shirota, Acc. Chem. Res. **40**, 1217 (2007).
[13] A. A. H. Pádua, M. F. C. Gomes, and J. N. A. C. Lopes, Acc. Chem. Res. **40**, 1087 (2007).
[14] A. Wulf, K. Fumino, and R. Ludwig, Angew. Chem., Int. Ed. **49**, 449 (2010).
[15] Y. Umebayashi, H. Hamano, S. Tsuzuki, J. N. A. C. Lopes, A. A. H. Pádua, Y. Kameda, S. Kohara, T. Yamaguchi, K. Fujii, and S. Ishiguro, J. Phys. Chem. B **114**, 11715 (2010).
[16] T. Masaki, K. Nishikawa, and H. Shirota, J. Phys. Chem. B **114**, 6323 (2010).
[17] K. Fujii, R. Kanzaki, T. Takamuku, Y. Kameda, S. Kohara, M. Kanakubo, M. Shibayama, S. Ishiguro, and Y. Umebayashi, J. Chem. Phys. **135**, 244502 (2011).
[18] J. L. Anthony, E. J. Maginn, and J. F. Brennecke, J. Phys. Chem. B **106**, 7315 (2002).
[19] X. Creary, E. D. Willis, and M. Gagnon, J. Am. Chem. Soc. **127**, 18114 (2005).
[20] A. Vidis, C. A. Ohlin, G. Laurenczy, E. Kusters, G. Sedelmeier, and P. J. Dayson, Adv. Synth. Catal. **347**, 266 (2005).
[21] C. Chiappe, P. Piccioli, and D. Pieraccini, Green Chem. **8**, 277 (2006).
[22] H. B. Zhao, J. E. Holladay, H. Brown, and Z. C. Zhang, Science **316**, 1597 (2007).
[23] H. Mehdi, A. Bodor, D. Lantos, I. T. Horváth, D. E. De Vos, and K. Binnemans, J. Org. Chem. **72**, 517 (2007).
[24] M. Ruta, G. Laurenczy, P. J. Dyson, and L. Kiwi-Minsker, J. Phys. Chem. C **112**, 17814 (2008).
[25] G. Yong, Y. Zhang, and J. Y. Ying, Angew. Chem., Int. Ed. **47**, 9345 (2008).
[26] Y. Yasaka, C. Wakai, N. Matubayasi, and M. Nakahara, J. Chem. Phys. **127**, 104506 (2007).
[27] M. Nakahara and C. Wakai, J. Chem. Phys. **97**, 4413 (1992).
[28] C. Wakai and M. Nakahara, Bull. Chem. Soc. Jpn. **69**, 853 (1996).
[29] J. McConnell, *The Theory of Nuclear Magnetic Relaxation in Liquids* (Cambridge University Press, Cambridge, 1987).
[30] J. A. Ingram, R. S. Moog, N. Ito, R. Biswas, and M. Maroncelli, J. Phys. Chem. B **107**, 5926 (2003).
[31] N. Ito, S. Arzhantsev, and M. Maroncelli, Chem. Phys. Lett. **396**, 83 (2004).
[32] H. Jin, G. A. Baker, S. Arzhantsev, J. Dong, and M. Maroncelli, J. Phys. Chem. B **111**, 7291 (2007).
[33] H. Jin, X. Li, and M. Maroncelli, J. Phys. Chem. B **111**, 13473 (2007).
[34] S. Arzhantsev, H. Jin, G. A. Baker, and M. Maroncelli, J. Phys. Chem. B **111**, 4978 (2007).
[35] Y. Yasaka, M. L. Klein, M. Nakahara, and N. Matubayasi, J. Chem. Phys. **134**, 191101 (2011).
[36] Y. Yasaka, M. L. Klein, M. Nakahara, and N. Matubayasi, J. Chem. Phys. **136**, 074508 (2012).
[37] G. Lipari and A. Szabo, J. Am. Chem. Soc. **104**, 4546 (1982).
[38] G. Lipari and A. Szabo, J. Am. Chem. Soc. **104**, 4559 (1982).
[39] J. H. Antony, A. Dolle, D. Mertens, P. Wasserscheid, W. R. Carper, and P. G. Wahlbeck, J. Phys. Chem. A **109**, 6676 (2005).
[40] W. R. Carper, P. G. Wahlbeck, J. H. Antony, D. Mertens, A. Dolle, and P. Wasserscheid, Anal. Bioanal. Chem. **378**, 1548 (2004).
[41] W. R. Carper, P. G. Wahlbeck, and A. Dolle, J. Phys. Chem. A **108**, 6096 (2004).
[42] P. G. Wahlbeck and W. R. Carper, Chem. Eng. Commun. **194**, 1160 (2007).
[43] T. M. Alam, D. R. Dreyer, C. W. Bielwaski, and R. S. Ruoff, J. Phys. Chem. A **115**, 4307 (2011).
[44] Y. Nishiyama, M. Fukuda, M. Terazima, and Y. Kimura, J. Chem. Phys. **128**, 164514 (2008).
[45] H. Tokuda, S. Tsuzuki, M. A. B. H. Susan, K. Hayamizu, and M. Watanabe, J. Phys. Chem. B **110**, 19593 (2006).
[46] The radius of HCOO$^-$ anion was estimated by using Chem 3D programs (Cambridge Scientific Computing).
[47] J. N. C. Lopes and A. A. H. Pádua, J. Phys. Chem. B **108**, 16893 (2004).
[48] J. B. Harper and R. M. Lynden-Bell, Mol. Phys. **102**, 85 (2004).
[49] A. Wulf, K. Fumino, D. Michalik, and R. Ludwig, ChemPhysChem **8**, 2265 (2007).
[50] K. T. Gillen and J. E. Griffiths, Chem. Phys. Lett. **17**, 359 (1972).
[51] R. P. W. Struis, J. de Bleijser, and J. C. Leyte, J. Phys. Chem. **91**, 1639 (1987).